

Noise transmission through duct divisions in air circuits, considered as three-port acoustic systems

Jorge L. Parrondo^{a,*}, Joaquín Fernández^b, Iván García^a, Eduardo Ruiz^a

^a*Departamento de Energía, Universidad de Oviedo, Campus de Viesques, 33203-Gijón, Spain*

^b*Departamento de Electrónica e Ingeniería Electromecánica, Universidad de Extremadura, 06071-Badajoz, Spain*

Received 1 December 2003; received in revised form 1 December 2005; accepted 21 February 2006

Available online 8 May 2006

Abstract

An experimental study is presented on the characterization of the noise transmission properties of the duct junctions used in ventilation and air-conditioning air circuits, assumed as three-port acoustic systems with plane-wave sound propagation. The procedure requires the measurement and post-processing of the transfer functions between the control signals of three loudspeakers, one at each branch, and the sound pressure signal recorded at six positions (two-microphone technique). The result is the scattering matrix, which contains three reflection coefficients and six transmission coefficients. Experiments were conducted on junctions of ducts with the same diameter, with three different deviation angles for the branch take-off. Besides, several different airflow conditions were imposed for each geometrical configuration. This paper describes the methodology used and the results obtained for the cases tested, and discusses the effect of the different factors involved in the noise transmission through the duct divisions.

© 2006 Elsevier Ltd. All rights reserved.

1. Introduction

Air circuits for ventilating or air-conditioning (HVAC) systems may conduct the noise generated at the fans or other sources towards the ventilated rooms. Usual regulations for thermal installations in buildings impose maximum background noise values for each room type, in terms of overall noise levels (dBA) or referred to RC or NC indexes. In order to meet the noise specifications, many air circuits have to include silencers, either reactive or purely dissipative. Optimal selection of the silencers at the design stage of the system, especially necessary for the low-frequency noise, requires the previous calculation of the noise levels induced in the ventilated rooms.

For an accurate determination of the sound propagated along a duct system, a complete wave analysis is needed, based on a set of sound wave generation and transmission properties for each of the elements of the system; these properties are complex functions of frequency, different for each acoustic wave mode, and dependent on geometry and airflow [1]. However, the noise through HVAC ducts is usually estimated by means of simpler sound power methods, that use data of the generation or attenuation of sound energy for each element and frequency band, such as the formulas and tables indicated by ASHRAE [2]. Calculations are

*Corresponding author. Fax: +34985182098.

E-mail address: parrondo@uniovi.es (J.L. Parrondo).

performed by accumulating sound energy attenuations and re-generations along the air circuit, with no account of sound reflections.

Terao et al. [1] verified the validity of the wave method on a small-scale laboratory circuit, by introducing the acoustic properties for each element determined for plane-wave mode from FEM or BEM numerical calculations (without airflow) [3] or from experimental measurements (fan aerodynamic noise) [4]. Then they extended the application of the method to a full-scale HVAC system, and compared the results with the predictions from a conventional energy method. They concluded that, when the ducts were rigid, the energy method could easily underestimate the outlet sound powers for thirds of octave bands by 10 dB. However, the predictions from both methods were similar when the ducts had 0.6 dB/m attenuation. This can be attributed to the longer paths along the circuit associated to the waves reflected at some elements, like elbows, terminals or duct divisions, and the corresponding greater duct attenuation.

This suggests that an alternative approach to take advantage of the simplicity of the energy methods and the availability of sound energy generation and attenuation data for many elements [2], and, at the same time, to improve their predictions, is to incorporate the sound energy reflections in the calculations, for instance by considering new sound sources at the reflection elements in a simple iterative procedure [5]. For such purpose, the reflection and transmission of sound energy through each element has to be considered for all the different incidence directions, similarly to the wave methods.

Hence, for elements like duct divisions, with three or more ports, a considerably large amount of data is needed, that exceeds the data indicated in the usual design guidelines for noise through HVAC systems. For branch divisions, ASHRAE [2] suggests to estimate the exiting noise by dividing the incident sound energy in proportion to the cross-sections of the air outlet ducts, without considering the influence of the sound frequency, the branch deviation angles nor the air flow-rate through the branches. However, the effects of the sound frequency and geometry configuration are clearly not negligible [1]. Besides, the air flow-rate through duct divisions is usually characterized by flow separation, big velocity gradients and turbulence generation, so that there is a significant aerodynamic sound production and, also, the sound reflection and transmission properties can be expected to become modified for sufficiently high air velocities. Bodén et al. [6] studied the influence of the airflow on the acoustic passive properties of 90° elbows with different curvature ratios, and they obtained small unsymmetrical modifications for Mach numbers equal to 0.06 and 0.09, though the study was restricted to a low-frequency span (up to about one-third of the first cut-on frequency). Similar conclusions were obtained by Rämmal and Åbom [7], who characterized the acoustic properties of an air terminal device.

An experimental investigation was undertaken to characterize the plane-wave transmission properties for several branch junctions with variation of the deviation angles and of the air flow-rate distribution. The cross-section of the ducts was circular with 160 mm in diameter for all cases. Tests were performed by means of the two-microphone technique for each branch, under imposition of controlled acoustic loads with loudspeakers, following the procedure of Lavrentjev et al. [8] for a two-port acoustic system. In the present case, each branch was considered as a three-port system with two state variables for each port: the entering and the exiting pressure waves. For such a system, the noise transmission properties are described by nine complex transfer functions, collected in the so-called scattering matrix. The procedure can be extended to obtain not only the sound transmission properties but also the noise generated aerodynamically at the element itself [7,8], but the latter was considered beyond the scope of the present study. This type of methodology has been previously applied to one- and two-port elements, to characterize fans [8], elbows [6] and terminals [7]. It was also applied to multi-port elements [9], to account for the sound transmitted from a fan in modes of order higher than the plane-wave mode.

This paper describes the theoretical basis of the study, the experimental set-up and procedure, and the results obtained for three branch deviation angles and four different airflow distributions through each of the branch divisions. These results clearly show a strong dependence of the sound transmission properties with respect to the frequency, and, to a lesser extent, with respect to the geometry and the airflow distribution.

2. Characterization method

If the elements under study are considered as invariant linear acoustic systems with three input/output ports, a , b and c , they can be fully described by means of six state-variables (two for each port). Since the final purpose is the prediction of the sound transmitted along the air circuits, assumed as plane waves, convenient

state-variables are the incident pressure waves (p_-) and the reflected pressure waves (p_+) at each port (Fig. 1). With these state variables, the equation that characterizes a three-port acoustic element, i.e., a duct junction with three branches, can be expressed as:

$$\begin{pmatrix} p_{a+} \\ p_{b+} \\ p_{c+} \end{pmatrix} = \begin{pmatrix} R_a & T_{ba} & T_{ca} \\ T_{ab} & R_b & T_{cb} \\ T_{ac} & T_{bc} & R_c \end{pmatrix} \begin{pmatrix} p_{a-} \\ p_{b-} \\ p_{c-} \end{pmatrix} + \begin{pmatrix} p_a^s \\ p_b^s \\ p_c^s \end{pmatrix} = \mathbf{M} \begin{pmatrix} p_{a-} \\ p_{b-} \\ p_{c-} \end{pmatrix} + \mathbf{V}. \tag{1}$$

In Eq. (1), \mathbf{M} , the scattering matrix, collects the passive properties of noise reflection and transmission for the incoming sound from each branch side, and \mathbf{V} , the source vector, represents the noise generated at the junction itself, mostly due to flow separation at the deviating branches and the corresponding turbulence production. The terms of the source vector \mathbf{V} are not usually important except for high air velocities and great deviation angles. The present study has been focused on the noise transmission properties alone, i.e., on the determination of the scattering matrix \mathbf{M} .

According to the model of Eq. (1), the noise transmission properties of a branch junction are characterized by nine complex parameters. The modulus of these parameters represents the fraction of the incident pressure at one port that becomes transmitted (or reflected) to any of the other ports of the branch junction (Fig. 2). For an ideal situation of sound with a large wavelength compared to the branch division dimensions, so that the plane-wave assumption stands virtually at the division section itself, the reflection and transmission coefficients can be easily obtained by considering mass conservation and pressure continuity at the division section [10]. If the volumetric acoustic impedances are equal for the three pipes (like in the present experimental study if the air velocity is neglected with respect to the sound velocity) then the reflection and transmission coefficients may be found to be 1/3 and 2/3, respectively, regardless the direction of sound incidence or other variables. In general, however, such situation may not be realistic, and the nine parameters of the scattering matrix \mathbf{M} will depend on the frequency, branch geometry and aerodynamic conditions as well.

In order to determine the scattering matrix \mathbf{M} with no disturbing influence from the source vector \mathbf{V} , the technique used by Lavrentjev et al. [8] has been applied for the present study. The method, once adapted to the three-port case, consists in imposing three controlled acoustic states, by means of three loudspeakers, each at one side of the branch. Each acoustic state corresponds to one of the loudspeakers emitting sound while the other two are disconnected. The elements of \mathbf{M} and \mathbf{V} are not altered by the external acoustic loads. Hence, denoting each acoustic state with a super-index I, II or III, Eq. (1) may be extended to:

$$\begin{pmatrix} p_{a+}^I & p_{a+}^{II} & p_{a+}^{III} \\ p_{b+}^I & p_{b+}^{II} & p_{b+}^{III} \\ p_{c+}^I & p_{c+}^{II} & p_{c+}^{III} \end{pmatrix} = \begin{pmatrix} R_a & T_{ab} & T_{ac} \\ T_{ba} & R_b & T_{bc} \\ T_{ca} & T_{cb} & R_c \end{pmatrix} \begin{pmatrix} p_{a-}^I & p_{a-}^{II} & p_{a-}^{III} \\ p_{b-}^I & p_{b-}^{II} & p_{b-}^{III} \\ p_{c-}^I & p_{c-}^{II} & p_{c-}^{III} \end{pmatrix} + \begin{pmatrix} p_a^s \\ p_b^s \\ p_c^s \end{pmatrix}. \tag{2}$$

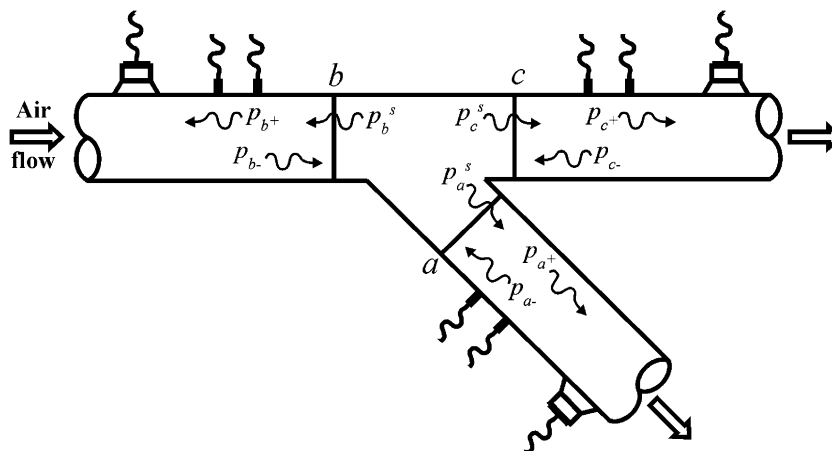


Fig. 1. A duct division as a three-port acoustic system, with a loudspeaker and two microphones on each duct.

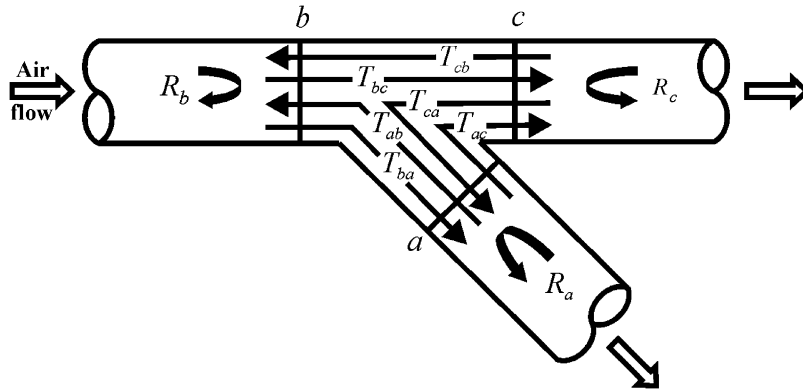


Fig. 2. Elements of the scattering matrix \mathbf{M} for the three-port acoustic system.

Assuming that the loudspeaker noise is not correlated with the aerodynamic noise generated at the duct junction, the transfer functions between the electric signal driving the active loudspeaker and the sound pressures of the source vector \mathbf{V} must be zero. In consequence, the source vector \mathbf{V} can be eliminated from Eq. (2) by considering not the sound pressure waves but the transfer functions H_e between the loudspeaker electric signals and those sound pressure waves:

$$\begin{pmatrix} H_{ea+}^I & H_{ea+}^{II} & H_{ea+}^{III} \\ H_{eb+}^I & H_{eb+}^{II} & H_{eb+}^{III} \\ H_{ec+}^I & H_{ec+}^{II} & H_{ec+}^{III} \end{pmatrix} = \begin{pmatrix} R_a & T_{ab} & T_{ac} \\ T_{ba} & R_b & T_{bc} \\ T_{ca} & T_{cb} & R_c \end{pmatrix} \begin{pmatrix} H_{ea-}^I & H_{ea-}^{II} & H_{ea-}^{III} \\ H_{eb-}^I & H_{eb-}^{II} & H_{eb-}^{III} \\ H_{ec-}^I & H_{ec-}^{II} & H_{ec-}^{III} \end{pmatrix}. \quad (3)$$

Eq. (3) represents a system of nine linear complex equations with nine complex unknowns, for each frequency. So, a solution can be easily obtained for each of the elements of the scattering matrix \mathbf{M} , in terms of the different transfer functions.

In order to use Eq. (3) in practice, the transfer functions involved in it must be referred to measurable magnitudes. However, a microphone does not capture the incident pressure waves (p_+) or the exiting ones (p_-), but the combination of both. This can be overcome by using two microphones (Fig. 1) for each of the branches a , b and c , at positions 1 and 2. For each branch, the pressure waves that travel either in the positive or in the negative direction pass at those two positions with a phase delay that is proportional to the separation distance and to the sound wavenumber. Following Lavrentjev et al. [8], if s_a , s_b and s_c are the separation distances of each microphone pair, k_{a-} , k_{b-} and k_{c-} are the wavenumbers of the incident sound at each branch, and k_{a+} , k_{b+} and k_{c+} are the wavenumbers of the exiting sound, the transfer functions of Eq. (3) can be referred to the measurable transfer functions by means of:

$$\begin{aligned} H_{ea+} &= \frac{H_{ea1} e^{ik_a s_a} - H_{ea2}}{e^{ik_a s_a} - e^{-ik_a s_a}}, & H_{ea-} &= \frac{-H_{ea1} e^{-ik_a s_a} + H_{ea2}}{e^{ik_a s_a} - e^{-ik_a s_a}}, \\ H_{eb+} &= \frac{H_{eb1} e^{ik_b s_b} - H_{eb2}}{e^{ik_b s_b} - e^{-ik_b s_b}}, & H_{eb-} &= \frac{-H_{eb1} e^{-ik_b s_b} + H_{eb2}}{e^{ik_b s_b} - e^{-ik_b s_b}}, \\ H_{ec+} &= \frac{H_{ec1} e^{ik_c s_c} - H_{ec2}}{e^{ik_c s_c} - e^{-ik_c s_c}}, & H_{ec-} &= \frac{-H_{ec1} e^{-ik_c s_c} + H_{ec2}}{e^{ik_c s_c} - e^{-ik_c s_c}}. \end{aligned} \quad (4)$$

Eq. (4) has to be successively applied for each of the three acoustic loads I, II and III (these super-indexes have been omitted in Eq. (4)). The air velocity along each of the branches can be introduced to obtain the effective sound speed and calculate the corresponding wavenumbers.

Eqs. (3) and (4) allow for the determination of the nine complex elements of the scattering matrix \mathbf{M} , as a linear function of frequency. However, the common practice for noise transmission calculations in ventilation and air-conditioning circuits is to consider the sound power propagated for each octave or third of octave frequency band [2]. For plane-wave acoustic propagation, the coefficients of sound power transmission or reflection for each frequency band can be estimated from the elements of the scattering matrix \mathbf{M} , as the

square of the modulus for the central frequency of that band. Then they can be converted to sound attenuations expressed in dB.

3. Experimental equipment and procedure

The methodology described above was put into practice with a series of laboratory tests to determine the sound power transmission properties of several duct junctions, varying the deviation angles and the airflow conditions. Three PVC pipes with 160 mm in internal diameter and a thickness of 4 mm were used for the branches of the test junction. At each pipe, at 3 m from the junction, a 6-in loudspeaker was mounted on a lateral opening with an inclination of 45° , without contracting the pipe cross-section. One of the branches was connected to the air supply system, which consisted of a centrifugal fan with an outlet cross-section of 400 mm in diameter, a dissipative silencer with several annular sound absorbent chambers of increasing external diameter, and a transition duct to reduce the cross-section to the 160 mm diameter (Fig. 3). The loudspeakers were controlled from a white noise signal generator. The silencer was inserted to reduce the fan noise well below the level of the loudspeakers sound pressure (about 100 dB), so that the signal averaging process at the measurement section could be reduced in time to a few minutes. The airflow distribution through the circuit could be altered by means of an obstruction plate at the end of each exit duct. Air velocity was measured at both outlets, at a number of radial and peripheral positions, with a Pitot tube connected to an inclined piezometric manometer. Mean velocity along the pipes was obtained from the average of those measured values, according to flow-rate measurement standards.

On each of the three branches, two 1/2-in microphones could be located flush-mounted, at 550 and 660 mm from the junction. These positions were chosen after testing several other microphone relative separations as well as several distances from the duct divisions, so that the useful frequency span of the measurements could extend along most of the plane-wave region, and, on the other hand, some space was given for both flow stream and sound waves to resettle after traversing the junction. A 01 dB Symphonie analyser was used to capture and process the sound pressure signals of the microphones, as well as the electric signals of the loudspeakers. During each test, the analyser produced the transfer functions between the three loudspeakers and the six microphone signals, with a frequency span from 250 to 1250 and 1.25 Hz of resolution (for some of the tests the span used was 300–1300 Hz). This span covers most of the frequency range with plane-wave transmission alone (for a pipe diameter of 160 mm the efficient sound propagation in the second mode begins at about 1250 Hz). The number of samples acquired from each signal was equal or greater than 200. The 18 transfer functions obtained at each test were then provided as input data for an especially designed calculation program. This program performed the calculations indicated in Eqs. (3) and (4) of the preceding section, to obtain the sound reflection and transmission coefficients of the scattering matrix \mathbf{M} .

In order to check the procedure, preliminary tests were conducted on a 90° squared bend, considered as a particular three-port acoustic system with one cancelled port (no entering or exiting sound at that port). The results showed very good agreement with the ASHRAE guidelines for sound transmission through elbows, which include the influence of frequency [2].

Additionally, for the cases of branch divisions with no flowing air, tests were conducted with the fan stopped and, also, with the fan in operation and both circuit exits closed. As expected, the results proved that the noise coming from the fan did not affect the measurement of the transfer functions between the loudspeaker and the microphone signals.

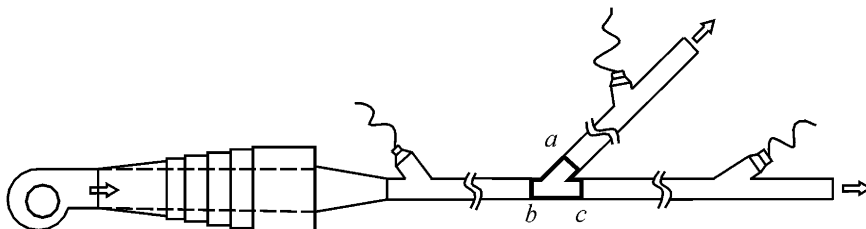


Fig. 3. Experimental set-up: fan, silencer and test air circuit, with duct junction and three loudspeakers.

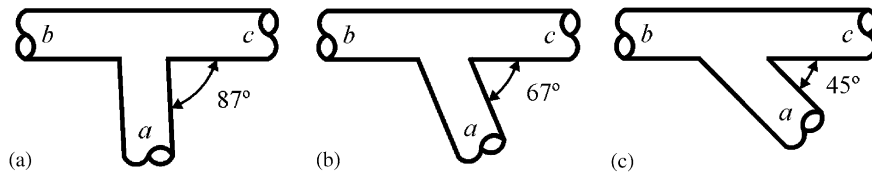


Fig. 4. Duct junctions tested.

Experiments were conducted on three commercial branch divisions with nominal deviation angles $\varphi = 45^\circ$, 67° and 87° , relative to the direction of the inlet duct (Fig. 4). In all cases, the designation used for the branches is: a = pipe take-off; b = airflow inlet; c = airflow outlet, aligned with duct b . For each geometry, four different airflow conditions were considered: (i) pipes a and c closed (no airflow); (ii) pipe a open and pipe c closed; (iii) pipe a closed and pipe c open; and (iv) pipes a and c open. Several series of tests were conducted for each geometry configuration and airflow condition. The data reported in the following sections were obtained from the average of the results for each case. From those sets of data, the uncertainty of the modulus of the elements of the scattering matrix \mathbf{M} for the no flow case was established in less than 4% for values greater than 0.4 and less than 7.5% for values above 0.2. For the cases with flowing air, the uncertainty was less than 6% for values greater than 0.4 and less than 12% above 0.2.

4. Experimental results with no flowing air

Fig. 5 presents nine diagrams, one for each of the sound reflection and transmission coefficients (modulus of the elements of the scattering matrix \mathbf{M}) obtained for the three deviation angles in the case of no airflow in the circuit. Each diagram relates the corresponding coefficient to the normalized angular frequency $\omega^* = 2\pi fD/c$, where f is the frequency, c the velocity of sound and D the pipe diameter.

As expected, at the lower frequency range all the curves tend towards the ideal values of $1/3$ for the reflection parameters or $2/3$ for the transmission parameters. However, the trends followed for increasing frequency values vary from one parameter to another. For the sound coming from the branch take-off, i.e., port a , the reflection coefficient R_a increases fast with the frequency, whereas the transmission coefficients T_{ab} and T_{ac} diminish. On the contrary, for the sound entering through port b , the reflection coefficient R_b reduces to very small values when increasing the frequency, whereas the transmission coefficient T_{ba} reduces and T_{bc} increases. Similar behaviour is observed for the sound entering through port c . The results obtained for $\varphi = 87^\circ$ are in good agreement with the predictions from finite element calculations reported by Terao [11] for a T-shaped rectangular duct junction with the same cross-section at the three branches. Altogether, the diagrams of Fig. 5 show that the scattering matrix \mathbf{M} is remarkably symmetric for this case of no airflow, which is a consequence of reciprocity since all the ducts have the same cross-section.

The effect of the deviation angle appears to be small when comparing the curves of Fig. 5 corresponding to $\varphi = 67^\circ$ and 87° , especially for the transmission coefficients. However, that effect becomes more significant when comparing the curves for $\varphi = 45^\circ$ and 67° : the former happen to be less steep with respect to the frequency. The differences in the transmission coefficients for both angles go up to 25% for high frequencies (equivalent to 2.5 dB in sound power attenuation). This variation is great enough to be worth considering it in the calculations of noise transmission along air circuits. The effect of the deviation angle is particularly evident in the reflection coefficients R_b and R_c . The latter, R_c , can be interpreted as the R_b coefficients for the angles $\varphi' = 180 - \varphi$ (i.e., $\varphi' = 93^\circ$, 113° and 135°). It may be observed from Fig. 5 that increasing the angle produces an increase in the frequency for which that reflection coefficient is a minimum. For the extreme case of $\varphi' = 135^\circ$, the reflection coefficient exhibits a maximum at about $\omega^* = 2.25$.

5. Experimental results with flowing air

Besides the no airflow case, three different airflow distributions were considered: flow from duct b to duct a (duct c closed), flow from duct b to duct c (duct a closed) and flow from duct b to both ducts a and c . The captions of Figs. 6–8 indicate the mean velocity of the air measured at pipes a and c for each deviation angle φ

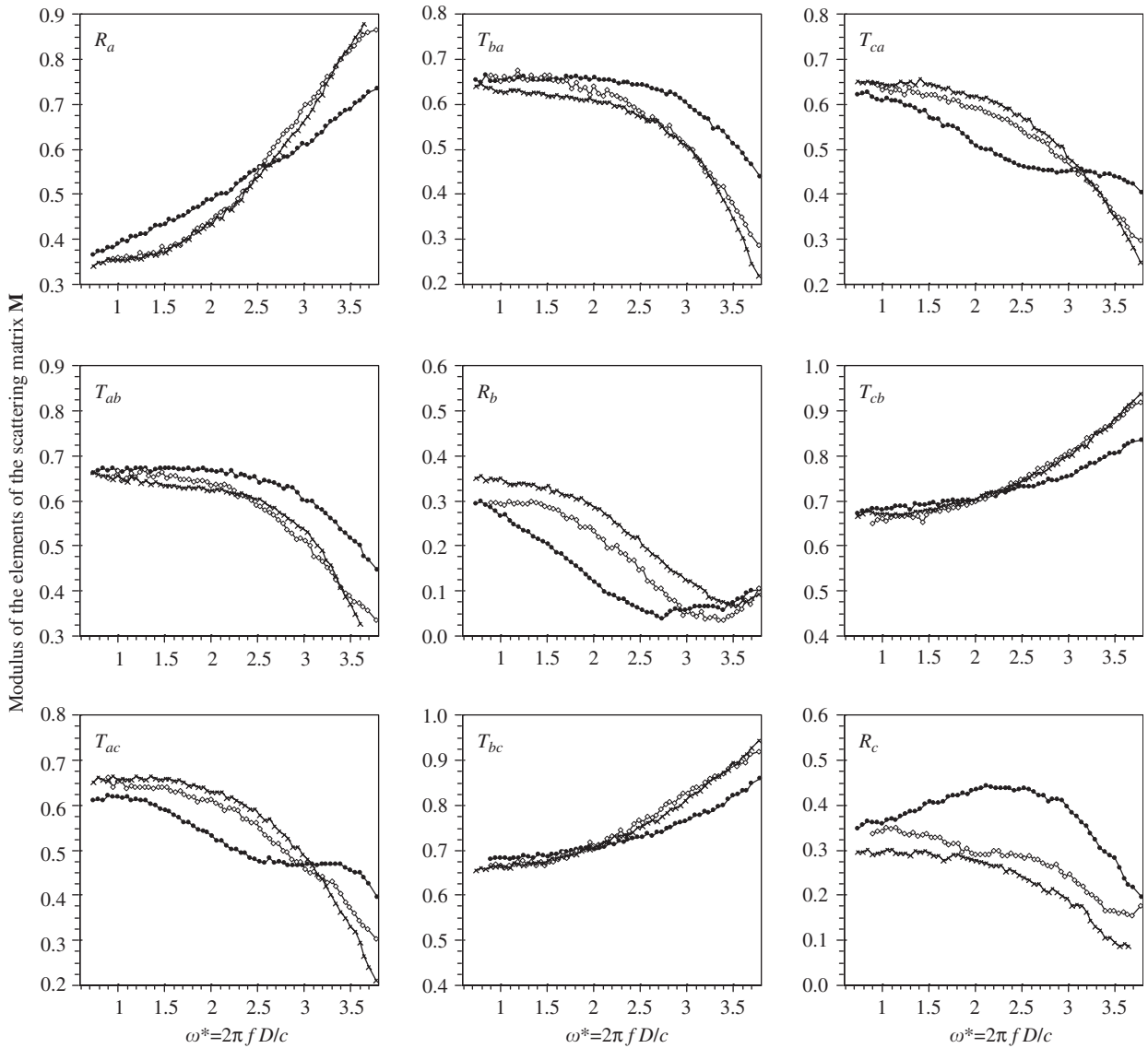


Fig. 5. Modulus of the elements of matrix \mathbf{M} for three deviation angles of the branch take-off and no flowing air, as a function of the normalized angular frequency ω^* . $\bullet\bullet\bullet$ 45°, $\diamond\diamond\diamond$ 67°, $\times\times\times$ 87°.

and airflow distribution; addition of the velocities at pipes a and c gives the velocity at pipe b , because the three pipes have the same cross-section. Most of these air velocities take values between 14 and 21 m/s, which can be considered a high range of velocities for usual ventilation circuits.

Figs. 6–8 present the results obtained, one for each of the three deviation angles tested. In these figures, each of the diagrams show the reflection or transmission coefficient corresponding to the no airflow case, considered as the reference case, together with the results for the three cases tested with flowing air. Though these new data present some scatter, many of the curves happen to be clearly shifted with respect to the no flowing air case, either positively or negatively, in more than 0.04 in modulus, which can be regarded as a quite appreciable effect. These shifts distort the symmetric appearance of the scattering matrix for the no flow case. On the other hand, when comparing any of the nine deviation parameters in Figs. 6–8, the effect of each airflow distribution appears to be very similar for the three deviation angles (the main exception to this rule is the reflection coefficient R_c , for high frequencies).

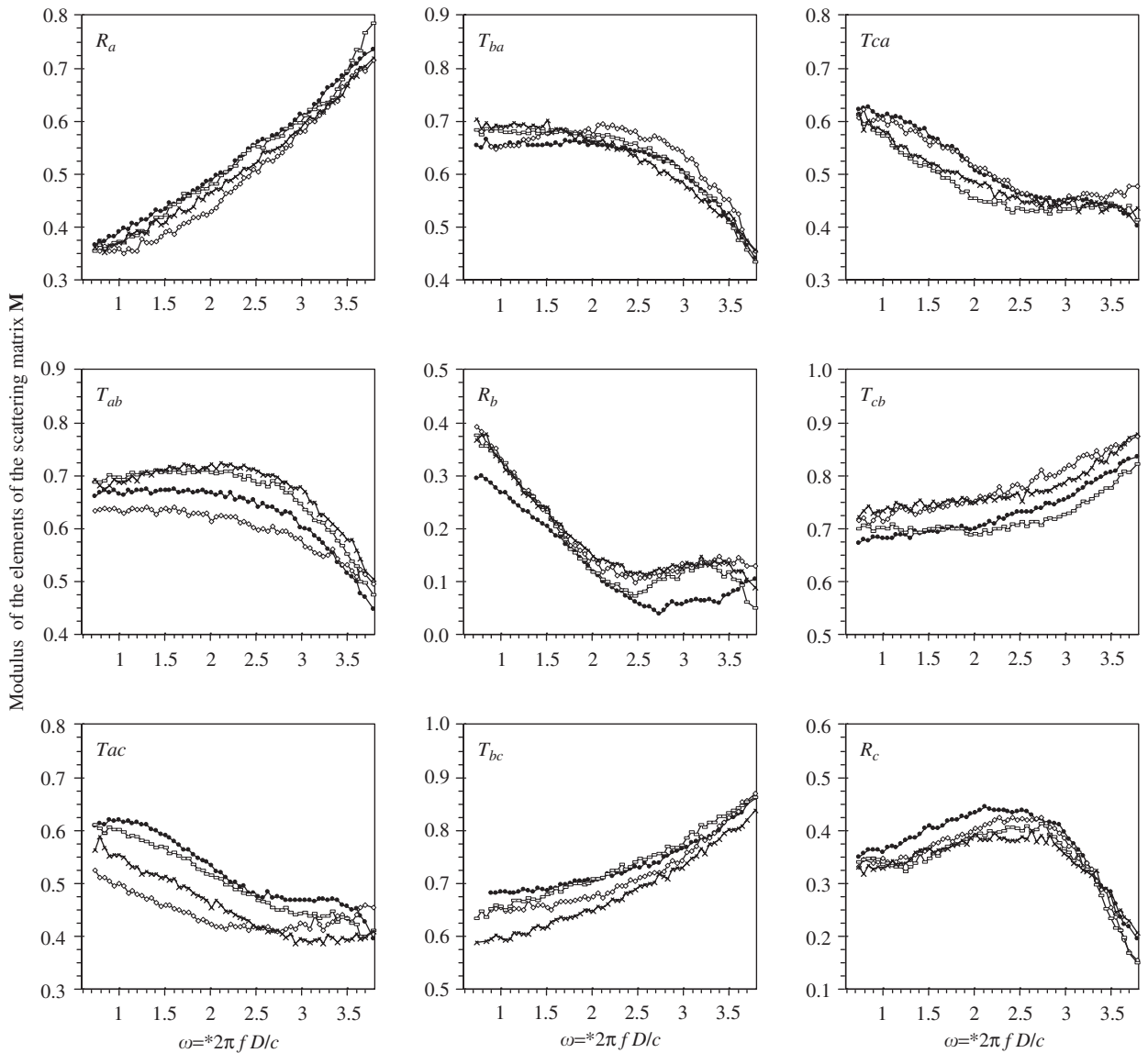


Fig. 6. Modulus of the elements of matrix \mathbf{M} with a deviation angle of 45° for the branch take-off and several airflow distributions. Flow velocities: $\bullet\bullet\bullet v_a = v_c = 0$; $\diamond\diamond\diamond v_a = 15.3 \text{ m/s}, v_c = 0$; $\square\square\square v_a = 0, v_c = 17.3 \text{ m/s}$; $\times\times\times v_a = 5.2 \text{ m/s}, v_c = 15.6 \text{ m/s}$.

For the first airflow distribution, when the air goes entirely from port b to port a , the abrupt change in flow direction at the branch division makes the flow to separate from the starting edge of duct a , forming a wake. Besides, duct c , which is closed, represents a lateral cavity, with flow separation as well. For this flow distribution, the three parameters associated to the noise entering through port a exhibit a significant reduction, especially for the low and middle range of frequencies. The greater reduction (more than 0.1 in modulus) corresponds to the T_{ac} parameter, for the three deviation angles. The reduction of these three parameters with respect to the no flow case implies that part of the sound energy entering at port a becomes dissipated. This dissipation is related to the presence of the wakes, where turbulence is generated and convected along the flow stream, because the acoustic waves impose some modulation on the unsteady wake pattern that leads to extra turbulence generation from acoustic energy extraction. Regarding the sound entering through port b , the transmission from port b to port a becomes augmented in about 0.04, whereas the transmission from port b to port c is reduced in a similar amount. Reflection at port b increases in some

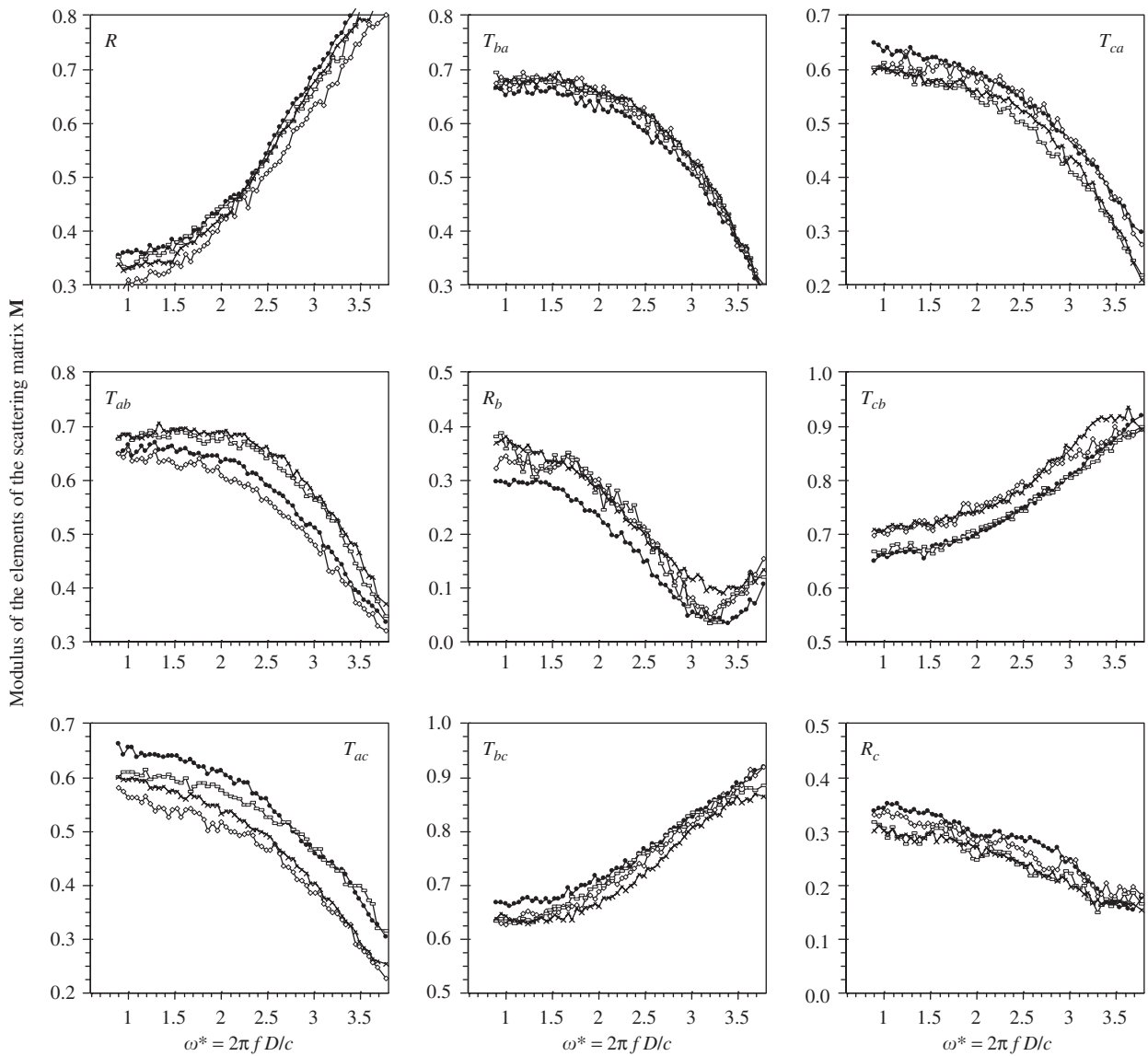


Fig. 7. Modulus of the elements of matrix \mathbf{M} with a deviation angle of 67° for the branch take-off and several airflow distributions. Flow velocities: $\bullet\bullet\bullet\bullet$ $v_a = v_c = 0$; $\diamond\diamond\diamond\diamond$ $v_a = 14.9$ m/s, $v_c = 0$; $\square\square\square\square$ $v_a = 0$, $v_c = 17.3$ m/s; $\ast\ast\ast\ast$ $v_a = 4.7$ m/s, $v_c = 15.9$ m/s.

amount for all frequencies (except for $\varphi = 87^\circ$ at high frequencies). Finally, the transmission of the sound entering through port c is not so much affected by the air flowing from pipe b to a : the transmission coefficient T_{cb} increases in about 0.04 except for $\varphi = 87^\circ$, T_{ca} remains always unchanged and the reflection coefficient R_c is seen to increase for $\varphi = 87^\circ$ at the higher frequency range.

When duct a is closed and all the air flows from duct b to duct c , the flow direction is unchanged and duct a acts as a lateral cavity, i.e., the flow separates from the wall of duct b and reattaches to the same wall, in duct c . Such a shear layer is usually unstable, acting like a source of turbulence that is convected along the main stream (duct c). For that reason, the effect of this airflow on the sound transmission coefficients is comparable to the previous case (air flowing only from port b to port a) after exchanging ports a and c , but the modifications with respect to the no airflow case are less pronounced. Significant modifications occur for the transmission coefficient T_{ca} , with reduction values of up to 0.05 at mid frequencies, the reflection coefficient

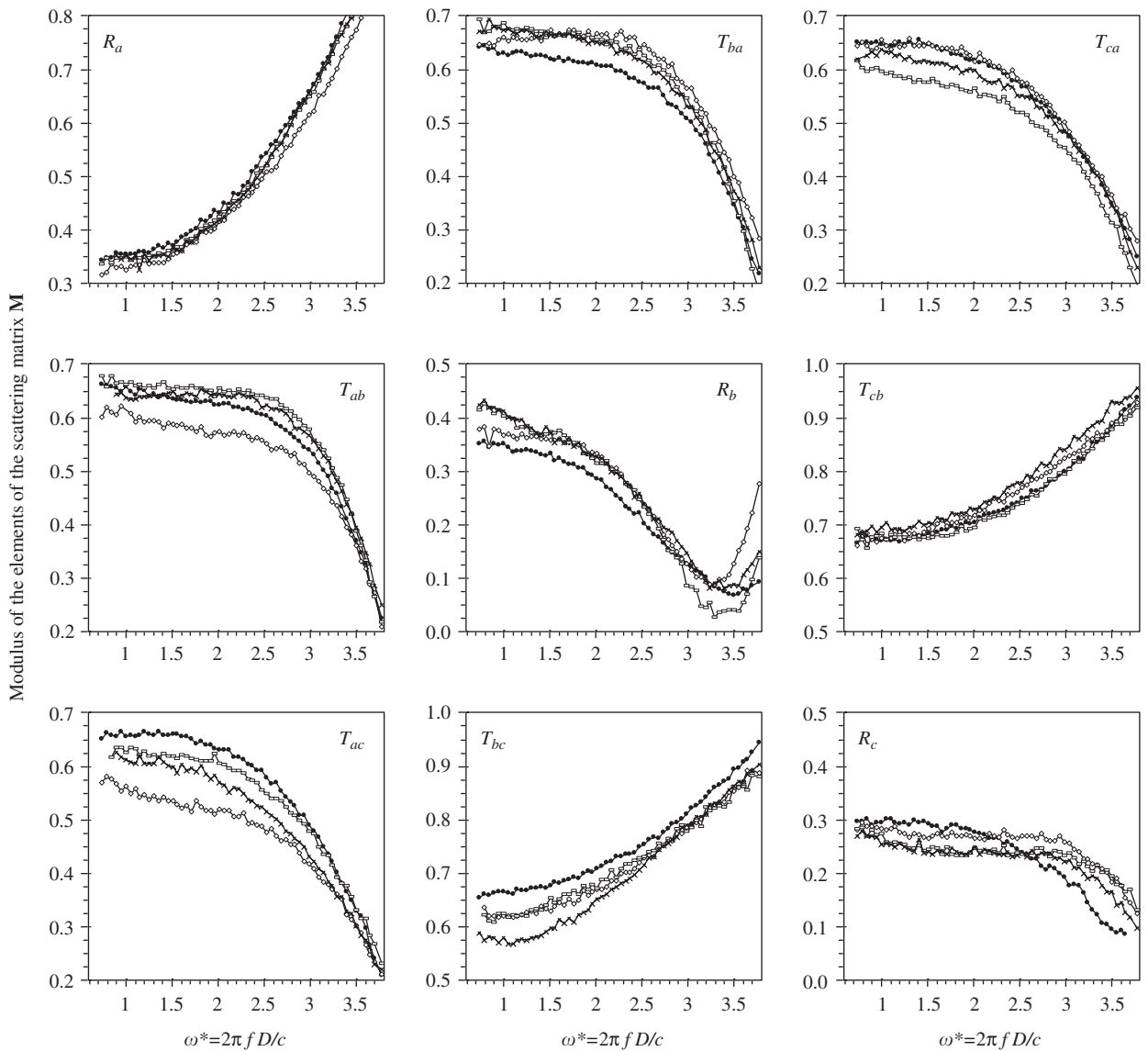


Fig. 8. Modulus of the elements of matrix \mathbf{M} with a deviation angle of 87° for the branch take-off and several airflow distributions. Flow velocities: $\bullet\bullet\bullet\bullet$ $v_a = v_c = 0$; $\diamond\diamond\diamond\diamond$ $v_a = 14.4$ m/s, $v_c = 0$; $\square\square\square\square$ $v_a = 0$, $v_c = 17.4$ m/s; $\times\times\times\times$ $v_a = 4.0$ m/s, $v_c = 16.3$ m/s.

R_c , that diminishes too in about 0.05, and the transmission coefficient T_{ab} , which increases in about 0.04. The coefficients associated to the sound entering through port b exhibit the same modifications with respect to the no flow case than with the previous airflow distribution, i.e., they are affected by the amount of air flowing through the port b itself, but not on the subsequent direction of the airflow.

In the third airflow distribution tested the air stream is actually divided at the junction and continues along both ducts a and c . Hence, this situation resembles some of the features of the two former flow distributions already considered. In particular the coefficients R_a , T_{ab} and T_{ac} , associated to the sound incident on port a , take values between the ones corresponding to the two preceding airflow cases. For the sound entering through port c , R_c and T_{ca} are equivalent to those coefficients in the case of duct a closed, whereas T_{cb} is equivalent to the same coefficient in the case of duct c closed. Finally, the coefficients associated to the noise entering through port b are very little changed from their values in the two former airflow situations.

For most of the cases tested, the variation in the reflection and transmission coefficients due to the presence of the airflow is within $\pm 12\%$ of the value for the no airflow case. The corresponding variation in the sound power attenuation is about 1 dB. The air velocities used in these tests correspond to a high range in practical air-circuits, and, hence, in many cases the effects of the flowing air will not be greater than in the present study. In consequence, it can be acceptable from an engineering point of view not considering the effect of the airflow when calculating the noise transmission through a branch junction. This result is in accordance with the conclusions from previous studies on the acoustic properties of elbows [6] and duct terminals [7].

6. Conclusions

An experimental study has been conducted to determine the sound transmission and reflection properties of branch take-offs in air-circuits, assumed as three-port acoustic systems with plane-wave sound propagation along the ducts. Experiments were conducted on junctions of tubes with the same diameter, for three deviation angles of the lateral branch and under different airflow conditions. The reported results are the modulus of the nine elements of the scattering matrix associated to a three-port system, with three reflection coefficients plus six transmission coefficients, and represent how the pressure waves incident on any of the ports become distributed among the exits. In order to incorporate these results in a standard power based method for calculation of HVAC noise, the squared magnitude of the acoustic transmission/reflection coefficients (Figs. 5–8) should be used for each frequency band.

The results show that, for the lower range of frequencies, the reflection and transmission coefficients tend towards the theoretical values of $1/3$ and $2/3$, respectively. However, they diverge very significantly from those values for high or even middle range frequencies. Some of those coefficients increase while others are reduced when augmenting the frequency, and, hence, the transmission of the noise through the junction depends strongly on the incoming and exiting sound directions considered. In general, the reflection coefficients are smaller but comparable in magnitude to the transmission coefficients (even greater for the case of the branch take-off at high frequencies), and hence the noise reflection at the junction is not to be considered negligible in general.

With respect to the deviation angle of the lateral branch, the reflection and transmission coefficients for a 45° deviation were found to vary with frequency more gradually than for the other two deviation angles. Differences in both reflection and transmission coefficients for the 45° angle with respect to the other two angles are usually of the order of 25%, i.e., 2.5 dB in terms of sound power attenuation, which is great enough to be worth considering it in the calculation of noise of air circuits. On the other hand, the effect of the flowing air was explored for the three branch deviations by directing all the airflow to one of the exits, to the other one or to both of them, with air velocities in the supply pipe up to 21 m/s. Most of the reflection and transmission coefficients were found to increase or decrease their values with respect to the no airflow case in less than 12%, i.e., less than 1 dB in terms of sound power attenuation. From an engineering perspective, these modifications can usually be considered small.

In summary, the results clearly indicate the great influence of the sound frequency and the incoming sound direction on the sound reflection and transmission coefficients of branch divisions, and they should be considered in the calculation of noise in air circuits. Though the deviation angle of the branch take-off has a smaller influence, it should also be taken in account in the calculations. On the contrary, the results of the study suggest that not considering the influence of the airflow distribution still will give results acceptable for engineering calculations in many practical cases.

Acknowledgements

The authors gratefully acknowledge the financial support of the Ministerio de Ciencia y Tecnología (Spain) under Projects DPI-00-0686 and DPI-02-04266-C02-02.

References

- [1] M. Terao, H. Sekine, M. Itoh, Comparison between wave theory and energy method in acoustic prediction of HVAC duct networks, *Proceedings of Building Simulation '99*, Vol. 3, Kyoto, Japan, 1999, pp. 1389–1396.
- [2] ASHRAE, *ASHRAE Applications Handbook, chapter 47: Sound and Vibration Control*, ASHRAE Inc., Atlanta, 2003.
- [3] M. Terao, H. Sekine, On substructure boundary element techniques to analyze acoustic properties of air-duct components, *Proceedings of INTER-NOISE 87*, Beijing, China, 1987, pp. 1523–1528.
- [4] M. Terao, H. Sekine, Fan acoustical characteristics required for reliable HVAC duct sound prediction, *Proceedings of the International Symposium on Fan Noise*, Senlis, France, 1992, pp. 343–350.
- [5] J.L. Parrondo, J. Fernández, D. Rodríguez, E. Alonso, Método de cálculo del ruido transmitido a lo largo de circuitos de aire, *Proceedings of the XXXII Congreso Nacional de Acústica*, Logroño, Spain, 2001, paper AAQ11.
- [6] H. Bodén, R. Glav, R. Ter-Riet, Measurement of sound transmission through a 90° bend with flow, *Proceedings of the Sixth International Congress on Sound and Vibration*, Vol. 1, Lyngby, Denmark, 1999, pp. 369–374.
- [7] H. Rämmal, M. Åbom, Characterization of air terminal device noise using acoustic 1-port source models, *Proceedings of the 10th International Congress on Sound and Vibration*, Vol. 1, Stockholm, Sweden, 2003, pp. 1829–1839.
- [8] J. Lavrentjev, M. Åbom, H. Bodén, A measurement method for determining the source data of acoustic two-port sources, *Journal of Sound and Vibration* 183 (1995) 517–531.
- [9] J. Lavrentjev, M. Åbom, Characterization of fluid machines as acoustic multi-port sources, *Journal of Sound and Vibration* 197 (1996) 1–16.
- [10] L.E. Kinsler, A.R. Frey, A.B. Coppens, J.V. Sanders, *Fundamentals of Acoustics*, third ed., Wiley, New York, 1982.
- [11] M. Terao, A method to estimate sound transmission losses in air-duct network including the contribution of reflected waves from discontinuities, *Proceedings of INTER-NOISE 86*, Cambridge, USA, 1986, pp. 571–576.